

# Novel Ni(II) and Zn(II) Schiff base metal chelates as promising DNA binder, Antioxidant and Antifungal agents

Anshita Varshney \*, and A. P. Mishra

Department of Chemistry, Dr. Hari Singh Gour Vishwavidyalaya (A Central University), Sagar, M.P. - 470003, India

**Abstract:** Schiff base ligands and their 3d-metal chelates have gained significant attention due to various applications in various scientific platforms. Due to their chelating propensity, they possess a wide range of biological, biochemical, catalytic, clinical, dying, and pharmacological properties. Here, in present studies, two novel Ni(II) and Zn(II) transition metal chelates have been synthesized by condensing their metal salts with Schiff base ligand 4-chloro-2-(2,5-dimethoxybenzylideneamino)-5-nitrophenol originated from 2,5-dimethoxybenzaldehyde and 2-amino-4-chloro-5-nitrophenol. The synthesized Schiff base ligand and its metal chelates have been Spectro-chemically examined by FT-IR, UV-Vis absorption spectroscopy, Mass Spectrometry, <sup>1</sup>HNMR, Thermogravimetric analysis (TGA) and Powdered-XRD. These compounds are biologically reactive and exhibit antifungal, antioxidant, and DNA-binding activity. The Ni(II) metal chelate gives better biological activity than the Zn(II) metal chelate and parent Schiff base ligand.

**Keywords:** Schiff base metal chelates; Spectroscopic characterization; Antifungal; Antioxidant; DNA binding property.

## 1. Introduction

The vast array of applications in many scientific platforms generates significant interest in Schiff base ligands and their coordinated transition metal chelates. These specialized ligands were studied due to their versatility, selectivity, and sensitivity towards the core metal atom. This makes them versatile actors in science and technology<sup>1-4</sup>. The azomethine (imine) group (-N=CH-) and other donor atoms, such as oxygen, nitrogen, sulfur, etc., facilitate the Schiff base ligand to chelate with metal ions<sup>5-7</sup>. Due to their chelating propensity, they display various applications in various fields. In bioinorganic chemistry, the binding capacity of the Schiff base ligand and its metal(II) complexes boost biological mechanisms' activity. It receives sufficient interest in the area of biological activity. These complexes behave like drugs (antibacterial, antifungal, antiviral, antihelminth, antimalarial, anticancerous, etc.) and play an essential role in medicinal biochemistry<sup>8-10</sup>. The advancement of organometallic chemistry has also dominated these moieties. The easy-made and easy-to-handle Schiff bases also exhibit many dyes, polymers, sensors, fluorescence, optical, biochemical, and nanomaterial properties<sup>11-12</sup>. Keeping the above in mind, the present

work's main objective was to deeply investigate this exciting field of study by creating and analyzing freshly synthesized Schiff base ligands and their coordinated transition metal complexes. Following an in-depth assessment of the literature, it has been revealed that no research had yet been done on the Schiff base ligand, which is produced from 2,5-dimethoxybenzaldehyde and 2-amino-4-chloro-5-nitrophenol and its Ni(II) and Zn(II) metal complexes. Various spectroscopic techniques have examined the compounds produced and screened for biological efficacy. The synthesized metal complexes show significant biological activities, which may be helpful as drugs in medicinal biochemical areas.

## 2. Experimental

**2.1. Materials and Method:** Reagents such as 2,5-dimethoxybenzaldehyde, Mol. Wt. 166.17 (99 % purity); 2-amino-4-chloro-5-nitrophenol Mol. Wt. 188.57 (99.9 % purity); Nickel chloride hexahydrate (NiCl<sub>2</sub>.6H<sub>2</sub>O: Mol.Wt. 237.69 g/mol; (99.9 % purity) and Zinc chloride dihydrate (ZnCl<sub>2</sub>.2H<sub>2</sub>O, Mol. Wt. 172.38 g/mol (99.8 % purity)) have been purchased from Merck-Sigma Aldrich, India of analytical grade. FT-IR spectra have been captured on BRUKER Alpha-II scientific FT-IR instrument, whereas LABINDIA

\*Corresponding author: Anshita Varshney  
 Email address: [anshitavarshney12@gmail.com](mailto:anshitavarshney12@gmail.com)  
 DOI: <http://dx.doi.org/10.13171/mjc02405211777varshney>

Received April 6, 2024  
 Accepted May 7, 2024  
 Published May 21, 2024

analytical UV-3092 Spectrophotometer has been used to measure UV-Vis absorption spectra of synthesized compounds.  $^1\text{H}$ NMR spectra have been measured on JEOL Delta-550 (400MHz Spectrometer) in  $d_6$ -DMSO. Thermal analysis of compounds has been done by using NETZSCH STA 449F1 instrument, up to 1000 K. Bruker D-8 Advances X-ray diffractometer has been used to capture the Powder-XRD patterns of synthesized samples at Centre for Advance Research (CAR), Dr. Harisingh Gour Vishwavidyalaya, Sagar (Madhya Pradesh), India. Mass spectra have been recorded on WATER'S Corporation, Model-Maldi-TOF Synapt XS HD Mass Spectrophotometer at SAIF, Panjab University, Chandigarh, India.

**2.2. Synthesis:** *Synthesis of ligand [DMCA]; 4-chloro-2-(2,5-dimethoxybenzylideneamino)-5-nitrophenol*: In a round bottom flask, methanolic solution of 2-amino-4-chloro-5-nitrophenol (3.77g, 20mmol) has been added dropwise with 2,5-dimethoxybenzaldehyde(3.32g,

20mmol) solution prepared in methanol(25ml) containing a bit of acetic acid as reaction stimulus<sup>13</sup>. The resulting reaction solution has been continuously heated with constant stirring on a magnetic hot plate stirrer at 50-60°C for 6-8 hrs. (Fig. 1). A shiny yellow precipitate has been separated and rinsed 2-3 times with modest amounts of methanol along with diethyl ether. After that, it was recrystallized with methanol and then dried over anhydrous  $\text{CaCl}_2$  in a vacuum environment.

Mol. Formula:  $\text{C}_{15}\text{H}_{13}\text{N}_2\text{O}_5\text{Cl}$ ; Mol. Wt.: 336.73; Yield: 82%; Color: Yellowish; M.P.: > 428 °C; stable; soluble in DMSO and DMF;

Anal. Calc.(%): C-53.50, H-3.89, N-8.32, O-23.76, Cl-10.53; Found(%): C-53.42, H-3.91, N-8.30, O-23.74, Cl-10.50; ;

FT-IR (selected vibrations,  $\text{cm}^{-1}$ ): 1635( $\nu_{\text{C}=\text{N}}$  azomethine), 1295( $\nu_{\text{C}=\text{O}}$ ), 3550-3700( $\nu_{\text{O}-\text{H}}$ ), Molar conductance (DMSO)  $\lambda_m$  ( $\text{Cm}^2\Omega^{-1}\text{mol}^{-1}$ ): 17.9.

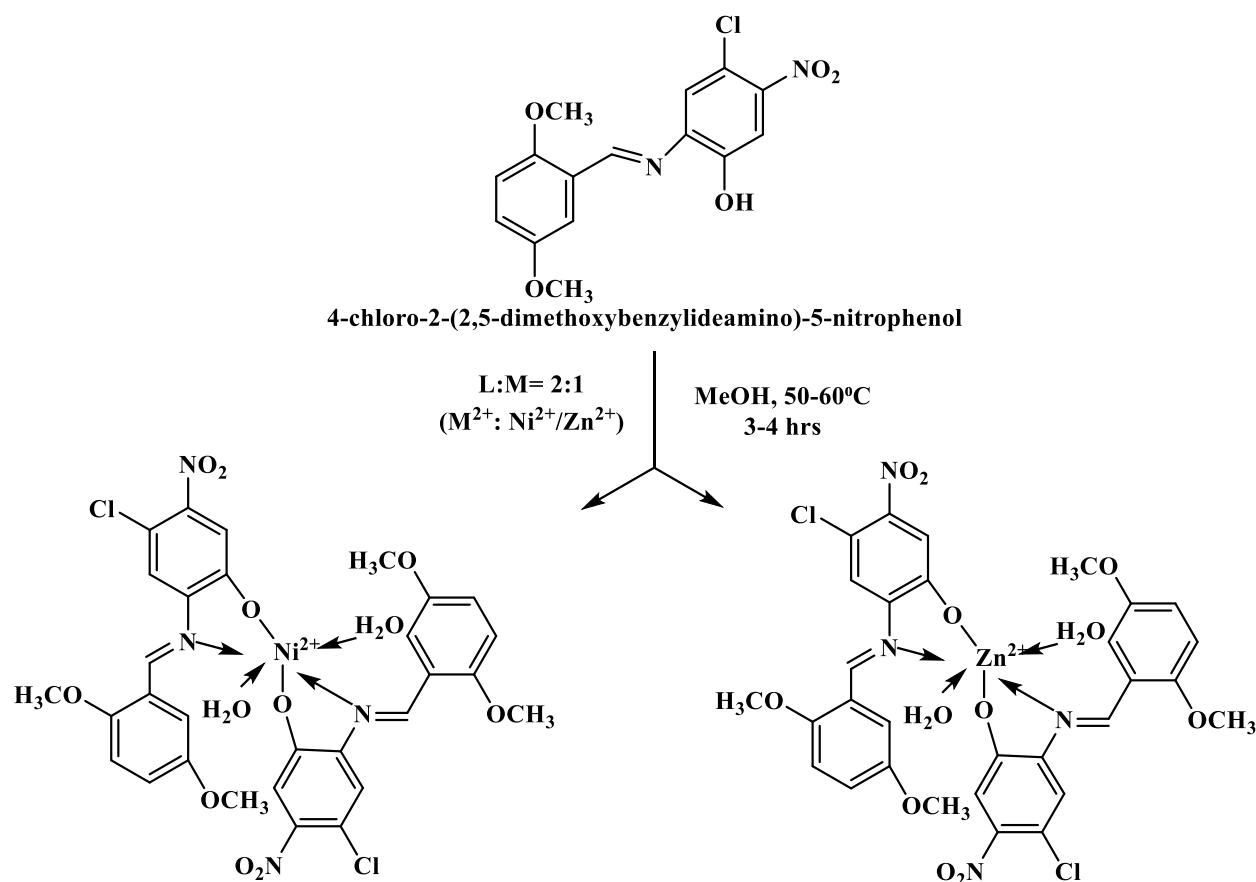


**Fig.1.** Projected synthesis scheme of DMCA (Ni/Zn) transition metal coordinated chelates

*Synthesis of Coordinated Metal Chelates*  $[\text{M}(\text{DMCA})_2 \cdot x\text{H}_2\text{O}] \cdot y\text{H}_2\text{O}$ ; (M: Ni(II) and Zn(II)): The two novel transition metal (II) coordinated chelates have been synthesized by refluxing 1mM of methanolic solution of individual metal (M: Ni(II)(0.237g) and Zn(II)(0.172g)) salts with methanolic solution of 2mM

of the ligand [DMCA (0.672g)] in slightly basic medium. The reaction combination has been continuously heated with constant stirring on a magnetic hot plate magnetic stirrer for 3-4 hrs. at 50-60°C. The TLC plate has detected the progress of the reaction. The colorful precipitates have been separated from each

reaction mixture and then rinsed 2-3 times with a modest mixture of methanol and diethyl ether, then recrystallized in methanol. The collected products have been placed in desiccators over anhydrous  $\text{CaCl}_2$  under a vacuum for drying.

$[\text{Ni}(\text{DMCA})_2 \cdot 2\text{H}_2\text{O}] / \text{DMCA-Ni}$ : Mol. Formula:  $\text{C}_{30}\text{H}_{28}\text{NiN}_4\text{O}_{12}\text{Cl}_2$ ; Mol. Wt.: 766.16; Yield: 78%; color: Dark green; Dec. temp.:  $> 455^\circ\text{C}$ ; stable; soluble in DMSO and DMF.

Anal. Calc.(%): C-47.03, H-3.68, N-7.31, O-25.06, Cl-9.25, Cu-7.66; Found(%): C-46.92, H-3.60, N-7.28, O-25.63, Cl-9.21, Cu-7.72;

FT-IR (selected vibrations,  $\text{cm}^{-1}$ ): 1628( $\nu_{\text{C=N}}$  azomethine), 483(M-N), 518(M-O); Molar conductance (DMSO)  $\lambda_m$  ( $\text{Cm}^2\Omega^{-1}\text{mol}^{-1}$ ): 26.8.

$[\text{Zn}(\text{DMCA})_2 \cdot 2\text{H}_2\text{O}] / \text{DMCA-Zn}$ : Mol. Formula:  $\text{C}_{30}\text{H}_{28}\text{ZnN}_4\text{O}_{12}\text{Cl}_2$ ; Mol. Wt.: 772.88; Yield: 74%; color: Brownish yellow; Dec. temp.:  $> 455^\circ\text{C}$ ; stable; soluble in DMSO and DMF.

Anal. Calc.(%): C-46.62, H-3.65, N-7.25, O-24.84, Cl-9.17, Cu-8.46; Found(%): C-46.72, H-3.61, N-7.30, O-24.50, Cl-9.32, Cu-8.28;

FT-IR (selected vibrations,  $\text{cm}^{-1}$ ): 1625( $\nu_{\text{C=N}}$  azomethine), 480(M-N), 518(M-O); Molar conductance (DMSO)  $\lambda_m$  ( $\text{Cm}^2\Omega^{-1}\text{mol}^{-1}$ ): 29.2.

### 3. Results and Discussion

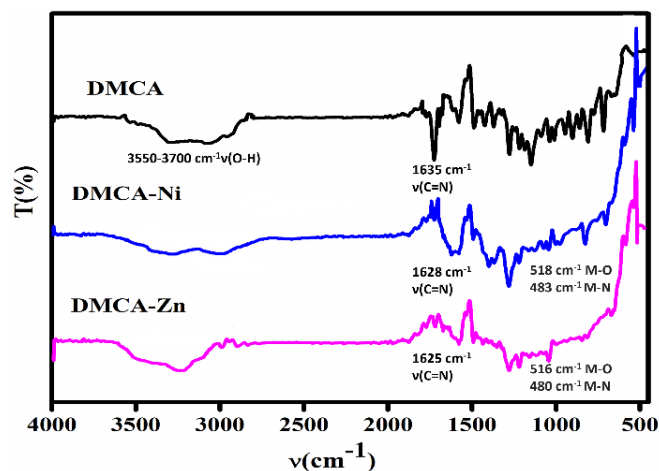


Fig. 2. FT- IR of DMCA and its transition metal chelates DMCA(Ni/Zn)

**3.1. Electronic absorption spectroscopy:** The absorption spectra of ligand DMCA has been observed at 270 nm and 362 nm, which corresponds to  $\pi \rightarrow \pi^*$  transition of aromatic ring and  $n \rightarrow \pi^*$  transition of azomethine (C=N) group. These absorption bands move to remarkably lower energies (longer wavelength) in both the complexes (276 nm and 372 nm for DMCA-Ni; 291 nm and 402 nm for DMCA-Zn). The electronic spectra of Ni(II) metal complex also show low-intensity d-d transition bands. The DMCA-Ni metal complex shows two bands at 471 nm ( $21505 \text{ cm}^{-1}$ ) and 675 nm

**Molar Conductivity:** At room temperature, the molar conductance of Schiff base ligand DMCA and its transition metal chelates DMCA(Ni / Zn) have been calculated in DMSO ( $5 \times 10^{-4} \text{ M}$ ). The calculated values of  $\lambda_m$  are  $17.26 \text{ cm}^2\Omega^{-1}\text{mol}^{-1}$  for DMCA,  $26.8 \text{ cm}^2\Omega^{-1}\text{mol}^{-1}$  for DMCA-Ni, and  $29.2 \text{ cm}^2\Omega^{-1}\text{mol}^{-1}$  for DMCA-Zn. These values verify the non-electrolytic nature of synthesized compounds.

**2.3. FT-IR spectroscopy:** FT-IR spectrum of ligand DMCA depicts some distinctive bands at  $1635 \text{ cm}^{-1}$  ( $\nu_{\text{C=N}}$ , azomethine),  $1295 \text{ cm}^{-1}$  ( $\nu_{\text{C-O}}$ ), and a specifically wide band at  $3550\text{-}3700 \text{ cm}^{-1}$  ( $\nu_{\text{O-H}}$ ). The movement of characteristic azomethine band to lesser frequency ( $1628 \text{ cm}^{-1}$  for DMCA-Ni and  $1625 \text{ cm}^{-1}$  for DMCA-Zn) and the appearance of new bands i.e. M-O ( $518 \text{ cm}^{-1}$  for DMCA-Ni and  $516 \text{ cm}^{-1}$  for DMCA-Zn) and M-N ( $483 \text{ cm}^{-1}$  for DMCA-Ni and  $480 \text{ cm}^{-1}$  for DMCA-Zn) stretching vibrations, respectively confirms the formation of metal complexes. The appearance of new additional bands of medium intensity at  $760\text{-}775 \text{ cm}^{-1}$  and  $630\text{-}668 \text{ cm}^{-1}$  regions correspond to  $\delta_r$  ( $\text{H}_2\text{O}$ ) rocking and  $\delta_w$  ( $\text{H}_2\text{O}$ ) wagging vibrations respectively, in both metal complexes, indicating the presence of coordinated water molecules in these complexes <sup>14-15</sup>. FT-IR spectra of synthesized compounds have been measured in DMSO Fig. 2.

( $14814 \text{ cm}^{-1}$ ), assignable to  ${}^3\text{A}_2\text{g}(\text{F}) \rightarrow {}^3\text{T}_{1\text{g}}(\text{P})$ ,  ${}^3\text{A}_2\text{g}(\text{F}) \rightarrow {}^3\text{T}_{1\text{g}}(\text{F})$  transitions respectively. This agreement favors the octahedral geometry of the complex. The DMCA-Zn metal complex does not show any d-d transition band due to  $d^{10}$  system. This alteration of  $\pi \rightarrow \pi^*$ ,  $n \rightarrow \pi^*$  transitions and d-d transition confirm the transformation of the molecular environment and the chelation of Schiff base ligand with transition metal ion <sup>16-17</sup>. UV-Vis spectra of synthesized compounds have been measured in DMSO (Fig. 3).

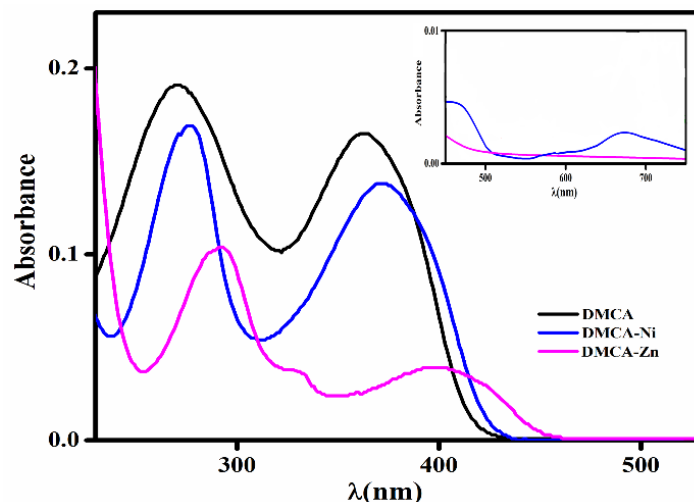


Fig. 3. UV-Vis absorption spectra of DMCA and its transition metal chelates DMCA(Ni/Zn)

**3.2.  $^1\text{H}$ NMR and Mass spectral studies:**  $^1\text{H}$ NMR spectral data of Schiff base ligand DMCA and its DMCA-Zn metal complex have been recorded in  $\text{DMSO-d}_6$ .  $^1\text{H}$ NMR spectral data of DMCA attributes 10.28(s,-OH), 7.62(s,-CH=N), 7.23-6.54(m, aromatic protons) signal peaks. While in the  $^1\text{H}$ NMR spectra of the  $[\text{Zn}(\text{DMCA})_2 \cdot 2\text{H}_2\text{O}]$  complex, the disappearance of the singlet peak at 10.28 reveals protonation of -OH during complex formation. On the other hand, the protons adjacent to coordination sites are shifted slightly to upfield (deshielding) i.e., 8.099(s, -CH=N) and 7.41-7.13 (m, aromatic protons)<sup>18-19</sup>. The  $^1\text{H}$ NMR spectral data have been shown in Fig. S1.

On the other hand, the ESI-MS spectra depict molecular ion peaks of DMCA and its metal-coordinated

complexes DMCA(Ni/Zn). By comparing the molecular formula weight with its  $m/z$  value in mass spectral data, the suggested molecular formula of each synthesized complex has been verified. The assigned molecular ion peak  $[\text{M}+2\text{H}]^+$  of DMCA was present at  $m/z$  338.33. Moreover, for metal complexes, the molecular ion peak  $[\text{M}-3\text{H}]^+$  at  $m/z$  763.61 assignable to entity  $[\text{Ni}(\text{DMCA})_2 \cdot 2\text{H}_2\text{O}]$ , and molecular ion peak  $[\text{M}+\text{H}]^+$  at  $m/z$  773.92 assignable to entity  $[\text{Zn}(\text{DMCA})_2 \cdot 2\text{H}_2\text{O}]$ . These isotopic peaks in ESI-MS spectral data also strongly support the making of ligand and metal complexes. The ESI-MS spectral data have been shown in Fig. S2.

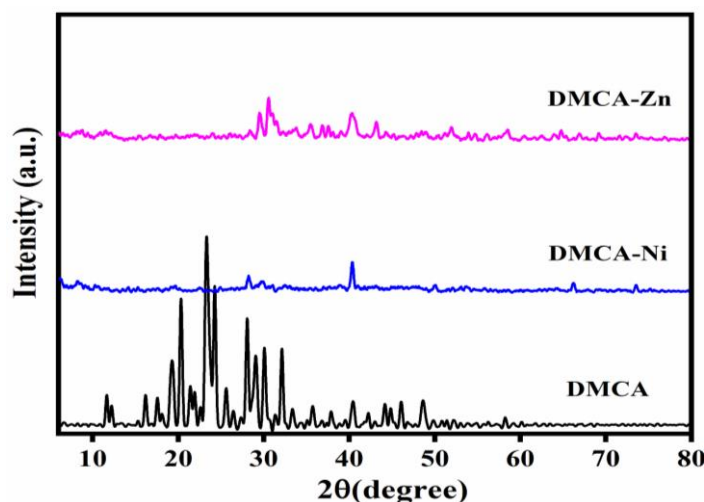


Fig. 4. Powdered- XRD pattern of synthesized compounds

**3.3. Powder X-ray diffraction and Crystallite size:** The synthesized compounds' structural information and materialistic properties have been measured using the powdered-XRD technique. The crystallite size of

particles in compounds has been calculated by using Scherre's equation<sup>20-21</sup> (eq. 1).

$$d_{\text{xrd}} = 0.9 \lambda / \beta \cos \theta \quad (1)$$

Where  $\lambda$  implies wavelength (Cu K $\alpha$ ),  $\beta$  implies full width at half maxima (FWHM), and  $\theta$  implies angle of diffraction. The inner crystal plane d-spacing parameters have been depicted by using Bragg's equation (eq. 2):

$$n\lambda = 2d\sin\theta \quad (n=1) \quad (2)$$

The diffractogram pattern of synthesized compounds has been shown in Fig. 4. The calculated data suggests that the ligand and its complexes exhibit a slightly crystalline nature. The most intensified peak ( $I_{\max}$ ) of HL<sub>3</sub> has been observed at 23.98° (2 $\theta$ ) with a 3.294 d-spacing value, for DMCA-Ni complex  $I_{\max}$  has been observed at 40.34° with a 3.232 d-spacing value, and for DMCA-Zn complex  $I_{\max}$  has been observed at 41.27°(2 $\theta$ ) with 3.121 d-spacing value. After using Scherrer's equation, the obtained crystallite size (dxrd) values for DMCA, DMCA-Ni, and DMCA-Zn are 21.3 nm, 18.9 nm, and 23.4 nm, respectively. The variation in diffraction angle, diffraction intensity, and the crystallite size of the ligand from its synthesized metal complexes suggest the formation of new complexes.

**3.4. Thermogravimetric analysis (TGA):** To analyze the stability of synthesized Schiff base transition metal coordinated chelates DMCA(Ni / Zn) against temperature, all the measurements have been done in the

N<sub>2</sub> atmosphere under 25 to 1000 °C temperature range, at 10°C min<sup>-1</sup> heating rate<sup>22-23</sup>.

The TGA graphs of synthesized metal chelates have been displayed in Fig. 5, which concludes the mass loss at different steps with temperature ranges, decomposition assignments, and final pyrolysis remaining product.

In the thermal graph of [Ni(DMCA)<sub>2</sub>.2H<sub>2</sub>O]; 5.98% (calc.5.94%) mass loss has been observed in the first step (35.35 – 94.83°C; DTG peak: 56.61°C), which corresponds to the elimination of two coordinated water molecules. In the second step (101.26 – 195.56°C; DTG peak: 165.92°C) decomposition of the non-chelated part of the organic moiety of synthesized Schiff base ligand in the metal complex is assignable to 11.46% (calc. 11.19%) of the total weight of the compound. The remaining non-chelating part, 25.50% (calc. 26.13%) of the organic moiety, has been eliminated in the third step (203.07 – 552.07°C; DTG peak: 469.19 °C). In the fourth step, 36.81% (calc. 36.74%) ranges from (558.72 – 872.31°C; DTG peak: 808.73°C) the chelated part of the organic moiety of Schiff base ligand has been decomposed. The final pyrolysis residue has been collected as Nickel (II) oxide NiO 17.44% (calc. 19.91%) along with carbide impurities and some by-products.

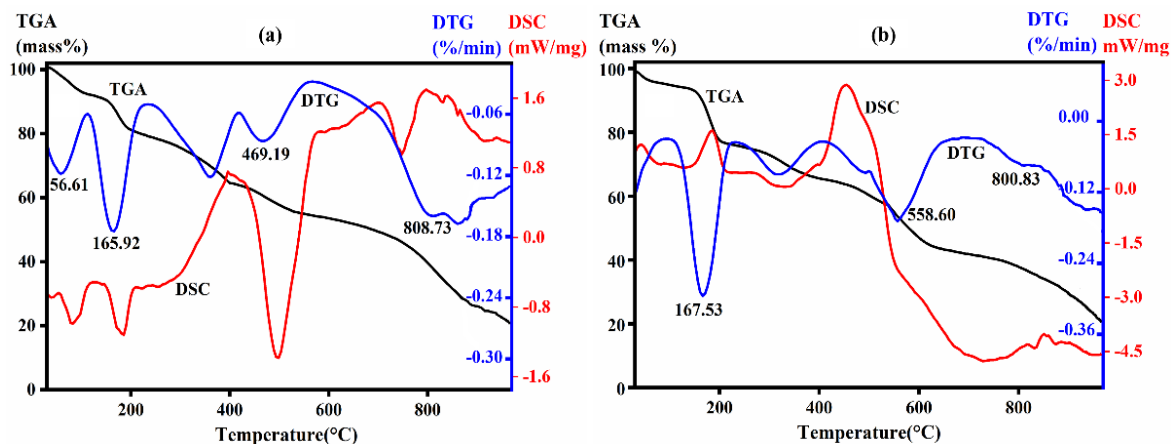


**Fig. 5.** Thermogram plots of (a)[Ni(DMCA)<sub>2</sub>.2H<sub>2</sub>O] and (b)[Zn(DMCA)<sub>2</sub>.2H<sub>2</sub>O] complexes

In the thermal graph of [Zn(DMCA)<sub>2</sub>.2H<sub>2</sub>O], 23.45% (calc.23.11%) mass loss has been observed in the first step (71.25 – 200.92°C; DTG peak: 167.53°C) corresponds to the elimination of two coordinated water molecules along with some non-chelating part of synthesized ligand. In the second step (206.28 – 641.19°C; DTG peak: 558.60°C), there is a decomposition of the remaining non-chelated part as well as some chelating part of the organic moiety of complex, assignable to 32.30% (calc. 32.59%) of the total weight of the compound. In the third step, 15.12%

(calc. 15.34%) ranging from (648.51 – 871.24°C; DTG peak: 800.83°C) assignable to the elimination of the remaining chelating part of the organic moiety of the complex. The final pyrolysis residue has been collected as Zinc(II) oxide ZnO 27.24% (calc. 28.71%) along with carbide impurities and some by-products.

### 3.5. Biological activities

**DNA Binding:** DNA is the most prevalent pharmaceutical molecule in cancer treatment. In the current study, using electronic absorption spectroscopy,

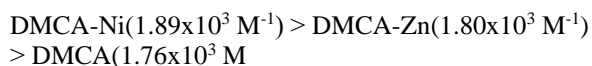
the DNA binding ability of synthesized Schiff base ligands and their transition metal complexes have been investigated against the pCAMBIA vector DNA. pCAMBIA DNA's (Circular DNA) stock solution was prepared by utilizing doubly distilled water with purity, having the coefficient of molar absorption ( $\epsilon = 6600 \text{ M}^{-1}/\text{cm}$ ) with its  $\lambda_{\text{max}}$  values at 260 and 280 nm (ratio of  $A_{260}/A_{280} > 1.8$ ). For spectrophotometric analysis, the concentrated stock solutions of synthesized compounds have been prepared in DMSO and diluted to the desired concentration using a Tris-HCl buffer solution. During analysis, the concentration of all the compounds was kept steady, with the successive increase in plasmid DNA concentration (from  $5 \times 10^{-5}$  -  $3 \times 10^{-4} \text{ M}$ ), and the most prominent band was used to calculate the alterations in absorbance. After the incubation period of 2 min at physiological pH 7.4, the solution was ready for photometric response. The binding constants ( $K_b$ ) of synthesized compounds have been calculated by using Wolfe - Shimer equation (eq. 3):

$$\frac{[\text{DNA}]}{(\epsilon_a - \epsilon_f)} = \frac{[\text{DNA}]}{(\epsilon_b - \epsilon_f)} + \frac{1}{K_b(\epsilon_b - \epsilon_f)} \quad (3)$$

Where  $[\text{DNA}]$  is the concentration of DNA's base pairs;  $\epsilon_a$ ,  $\epsilon_f$ , and  $\epsilon_b$  are  $A_{\text{obs}} / [\text{complex}]$  (i.e., the apparent absorption coefficients, extinction coefficient for free compound under study, and extinction coefficient of the compound when completely bound to DNA, respectively). From the ratio of the slope to intercept of **Competitive binding studies**: In a fluorescence quenching experiment, the interaction between the synthesized chemicals and pCAMBIA DNA has been further investigated and quantified using Ethidium Bromide (EB). The fluorescence intensity of the EB+DNA complex decreases in the presence of testing chemicals (competitor binding agents prepared in DMSO ( $5 \times 10^{-4}$ )), the fluorescence intensity of EB+DNA complex reduces, which is due to the replacement of EB from EB+DNA complex by the competitor binding molecule. Emission spectra of the

plots  $[\text{DNA}] / (\epsilon_a - \epsilon_f)$  vs  $[\text{DNA}]$  binding constant,  $K_b$  was obtained<sup>24-26</sup>.

**DNA binding** with metal chelates produces the hyperchromic or hypochromic effect, regardless of the hypochromic or bathochromic impact during the absorption spectrum. The electrostatic binding mode is responsible for the hyperchromic effect, while the intercalative binding mode is responsible for the hypochromic effect. A distinct Schiff base ligand DMCA absorption band has been spotted in the UV region at 362 nm. In addition to pCAMBIA DNA to ligand, an observable hypochromic shift (peak with decreased intensity) is detected in the absorption band. The strong absorption band of DMCA-Ni observed at 372 nm, including pCAMBIA DNA to Ni-complex, has a remarkable hyperchromic effect (peak with increased intensity) in the UV region. The strong absorption band of the DMCA-Zn complex was observed at 402 nm, and a remarkable hypochromic shift (peak with decreased intensity) was detected by including pCAMBIA DNA in the Zn complex. The DNA binding potency of all the synthesized compounds has been shown in Fig. 6. The Binding constant  $K_b$  ( $\text{M}^{-1}$ ) obtained from the Wolfe - Shimer equation has been concluded in Table 1. It follows the order:



solutions were recorded in the range of 500–800 nm ( $\lambda_{\text{exc}} = 510 \text{ nm}$ ) after 5 min of incubation. The quenching constant  $K_{\text{SV}}$  has been measured by using the classical Stern-Volmer equation,  $I_0/I = 1 + K_{\text{SV}} [Q]$ , where  $I_0$  and  $I$  were the emission intensity in the absence and presence of the quencher (metal complexes), respectively, and  $[Q]$  was the concentration of the quencher<sup>27-28</sup>. The emission spectra of EB+DNA quenched by tested synthesized compounds have been given in Fig. 6. The quenching constants ( $K_{\text{SV}}$ ) obtained from Stern-Volmer plots have been concluded in Table 1.

**Table 1.** Electronic absorption spectral studies of synthesized Schiff base ligand DMCA and its metal complexes DMCA(Ni/Zn) with DNA.

Compounds	$\lambda_{\text{max}}(\text{nm})$		$\Delta\lambda$ (nm)	**Binding Constant $K_b$ ( $\text{M}^{-1}$ )	***Quenching constant $K_{\text{SV}}(\text{M}^{-1})$
	Free	Bound			
DMCA	362	363	1	$1.76 \times 10^3$	$4.8 \times 10^3$
DMCA-Ni	372	373	1	$1.89 \times 10^3$	$7.1 \times 10^4$
DMCA-Zn	402	403	1	$1.80 \times 10^3$	$5.2 \times 10^3$

Error limit  $\pm 2\%$ ; \*\* $K_b$  = Intrinsic DNA binding constant; \*\*\*  $K_{\text{SV}}$  = EB+ DNA Quenching constant

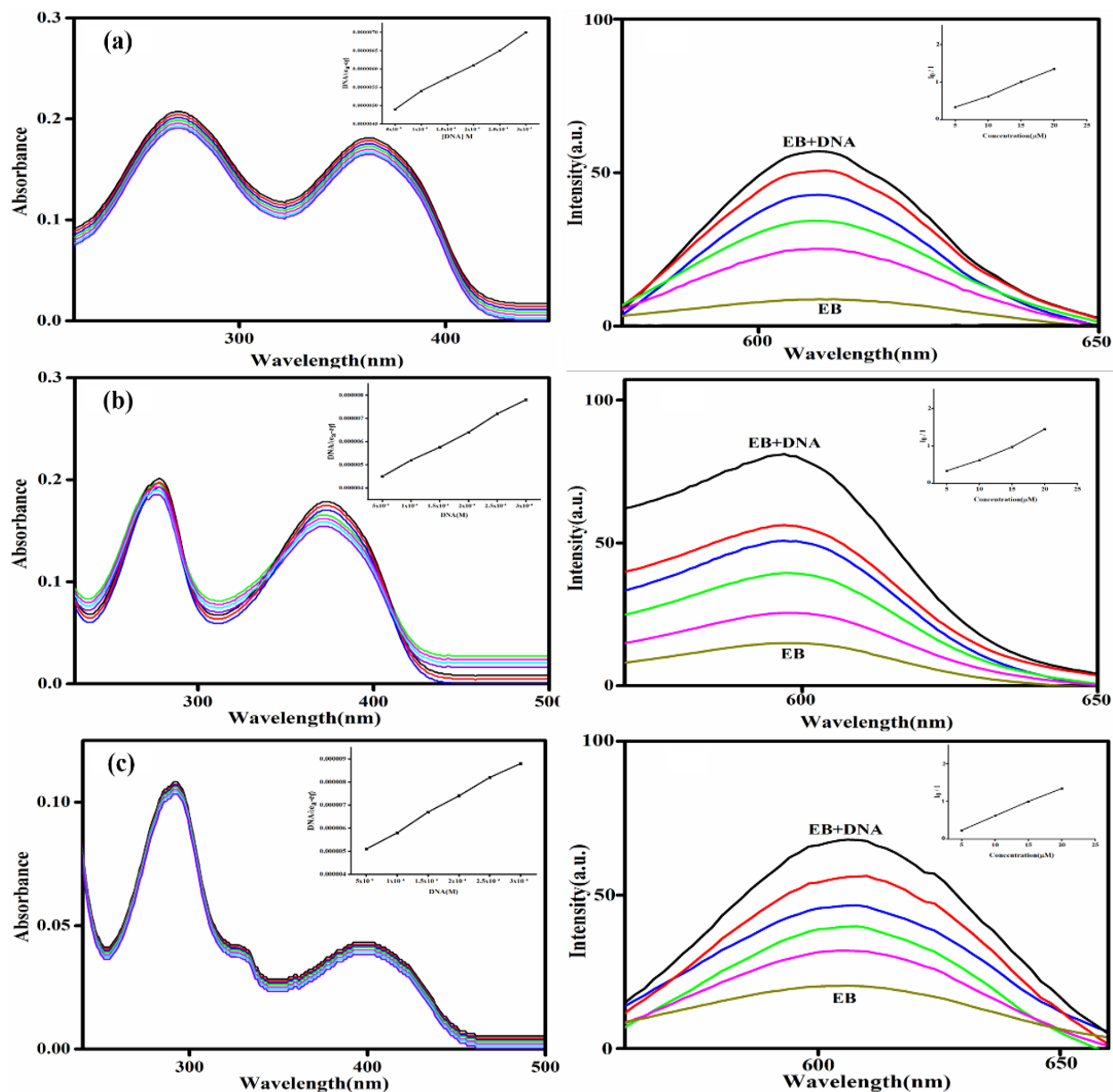


Fig. 6. Electron absorption spectrum and Fluorescence emission spectrum of a) DMCA, (b) [Ni(DMCA)<sub>2</sub>.2H<sub>2</sub>O] and (c) [Zn(DMCA)<sub>2</sub>.2H<sub>2</sub>O]

**3.6. Antifungal activity:** The fungal growth inhibition approach has been used to evaluate the inhibitory effect of the Schiff base ligand DMCA and its coordinated transition metal(II) complexes DMCA(Ni/Zn) against the two fungal species *Aspergillus niger* and *Fusarium oxysporum*<sup>29</sup>. In order to quantify the antifungal activity, 2 % autoclaved Dextrose Agar of Potato (PDA) media has been distributed into Petri plates of 9 cm diameter. Standard solutions of the tested samples (1mg/ml) have been prepared in 100% dimethyl sulfoxide (DMSO). After that, a specific volume of the stock solutions have been added separately to the set of Petri plates together with PDA media to attain a final

concentration of 100 μg/ml. After the solidification of media, a piece of 1.5mm (cut from the actively growing margin) of 7 days-old-fungal culture was placed as a central inoculum. Fungal growth has evaluated by measuring the diameter of the colony in cm after 7 days of incubation at an absolute 25°C temperature. The reduction percentage of growth has been calculated in contrast with the controlled growth (free from complexes), using the % Growth Inhibition equation (eq. 4):

$$\% \text{ Growth Inhibition} = \frac{D_0 - D_t}{D_0} \times 100 \quad (4)$$

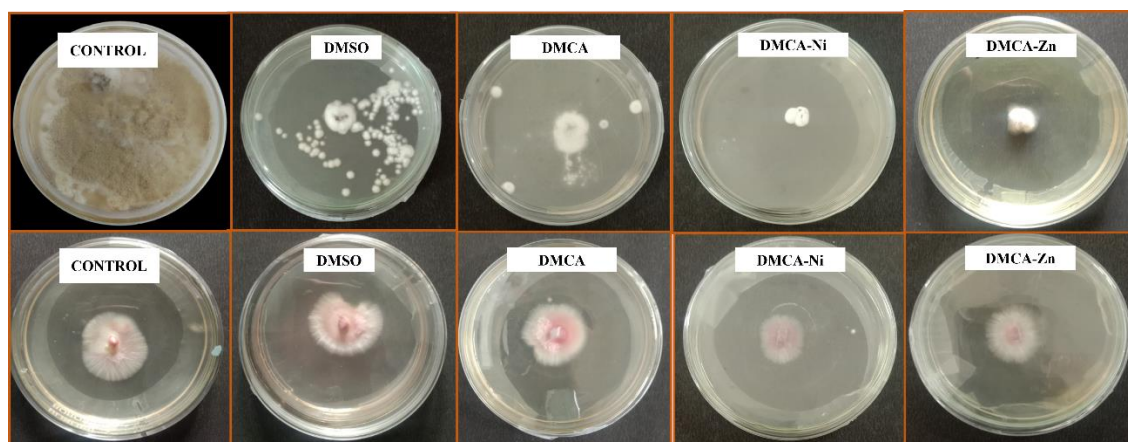
Where  $D_t$  is the fungal growth diameter with different treatments and  $D_o$  is the fungal growth diameter with control.

There is a decline in the fungal colony ground of various treatments and the controlled treatment observation.

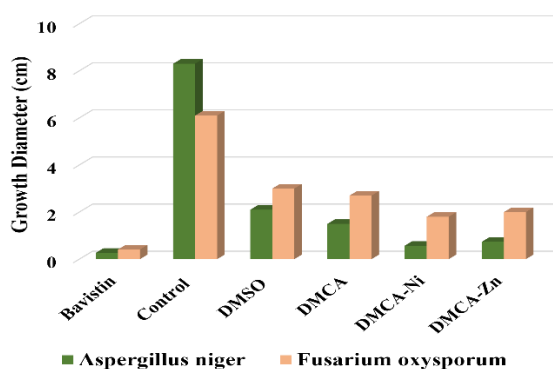
The metal complexes are commonly more effective against fungal strains than the parent ligand<sup>30</sup>. It has been concluded from Fig. 7(a, b) and Table 2 that the Ni(II) complex displayed good potency in contrast with Zn(II) complex and ligand against the fungal growth.

**Table 2.** Growth inhibition % of Schiff base ligand DMCA and its metal complexes DMCA(Ni/Zn) against the two fungal species *Aspergillus niger* and *Fusarium oxysporum*.

Compounds	Growth Inhibition %	
	<i>Aspergillus niger</i>	<i>Fusarium oxysporum</i>
Bavistin	98.06	92.19
Control	5.2	28
DMSO	74	48
DMCA	82.3	55
DMCA-Ni	92.2	81
DMCA-Zn	85	61.8



(a)



(b)

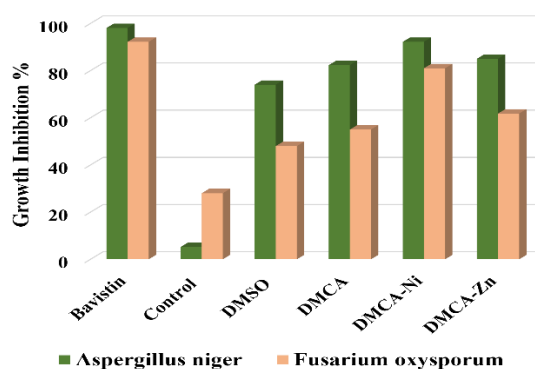


**Fig.7(a)** Pictorial demonstration of antifungal activity and **(b)** Graphical demonstration of inhibition % Growth of Schiff base ligand DMCA and its metal complexes DMCA(Ni/Zn), against the two species of Fungi *Aspergillus niger* and *Fusarium oxysporum*

**3.7. Antioxidant activity:** Due to oxidative imbalance, free radicals are generated in the body and play a significant role in oxidative damage of proteins. Antioxidants help capture and neutralize free radicals, protecting the body from harmful effects. In the present study, DPPH has been used to compare the antioxidant ability of the Schiff base ligand and its metal complexes. Ascorbic acid has been employed as a positive control. The capability to scavenge free radicals by synthesized compounds has been calculated using the methanolic solution of DPPH (2,2-diphenyl-1-picrylhydrazyl). The 0.1ml (100 $\mu$ L) solution of synthesized compounds at various concentrations (5, 10, 15, 20, 25 mg/L in DMSO) was added to 3.9 mL freshly prepared DPPH solution. These separately prepared mixtures of DPPH and the respective compound were shaken up and permitted to rest in the dark for 30 min at room temperature. At a respective wavelength of 517 nm, the absorbance has been recorded against the control solution. The radical scavenging capability of tested complexes has been expressed as the inhibition percentage of DPPH and is measured by using the Inhibition % equation (eq. 5):

$$\text{Inhibition (\%)} = \frac{A_{\text{control}} - A_{\text{sample}}}{A_{\text{control}}} \times 100 \quad (5)$$

$A_{\text{control}}$  is the absorbance of reaction with control (containing DMSO and DPPH solution), and  $A_{\text{sample}}$  is the absorbance of reaction with tested complex (containing test sample with DMSO and DPPH solution). Testing has been done in triplicate<sup>31</sup>. The free radical scavengers help reduce radicals, which decolorizes the color of the DPPH solution to light yellow from deep violet. The reduction in the degree of absorbance is the principal indication of antioxidant activity. A lower IC<sub>50</sub> value indicates higher antioxidant activity. The inhibition % has been calculated by using eq. 5. The scavenging abilities of synthesized compounds have been noted in order: Ascorbic acid > DMCA-Ni > DMCA-Zn > DMCA, as shown in Fig. 8. According to the results, it is concluded that DMCA-Ni complex gives the better activity than the others. From the literature survey, it is concluded that the antioxidant ability depends on various functional groups attached, conjugation, ionization potential, and reactivity of the nature of the ligand and its metal complexes<sup>32</sup>.

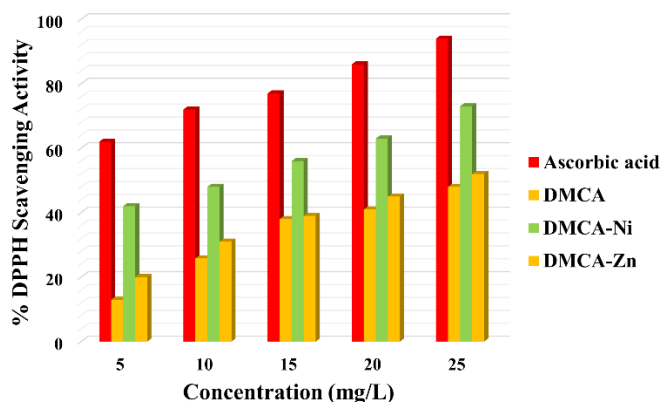


**Fig. 8.** DPPH Scavenging capacity of Schiff base ligand DMCA and its metal complexes DMCA(Ni/Zn) in DMSO

#### 4. Conclusion

After all the above findings, it has been concluded that the condensation of newly synthesized Schiff base ligand DMCA with Ni(II) and Zn(II) metal ion salts, consequences in the creation of two new mononuclear coordinated transition metal complexes having probably the distorted octahedral molecular geometry. The spectral characterization of synthesized compounds explains their structural arrangements. TGA analysis depicts the general decomposition pattern and the complexes' thermal stability. P-XRD spectral pattern defines synthesized compounds' slight crystalline nature and nanometer grain particle size. Using UV-Vis absorption spectroscopy, the DNA binding affinities of synthesized compounds towards pCAMBIA DNA shows that the DMCA-Ni metal complex displays good DNA binding efficacy. The DMCA-Ni(II) metal

complex also exhibits potent antifungal (against *Aspergillus niger* and *Fusarium oxysporum*) as well as effective antioxidant activity in comparison to DMCA-Zn(II) metal complex and parent Schiff base ligand DMCA. The biological activities concluded that the metal complexes depict noteworthy biological activities compared to the parent Schiff-base ligand. The outcomes may be helpful to as drugs in biomedical areas.

#### Acknowledgment

We thank the Department of Chemistry, Dr. H. S. Gour Vishwavidyalaya, Sagar India, for the FT-IR and UV-Vis spectroscopy facilities. We thank the Centre for Advance Research (CAR), Dr. H. S. Gour Vishwavidyalaya, Sagar, for <sup>1</sup>HNMR, Thermal analysis and P-XRD facilities. We thank SAIF, Panjab

University, Chandigarh, India, for mass spectral analysis. We thank the Head Department of Biotechnology, Dr. H. S. Gour Vishwavidyalaya, Sagar India, for the DNA binding activity facility. We thank the Head Department of Botany, Dr. H. S. Gour Vishwavidyalaya, Sagar India, for providing the antifungal activity facility. We thank UGC, New Delhi, India, for financial assistance through a non-NET fellowship.

### Conflict of interest

We have no conflict of interest in India or abroad.

### Reference

1. A. M. Abu-Dief, N. H. Alotaibi, E. S. Al-Farraj, Hamza A. Qasem, S. Alzahrani, M. K. Mahfouz, A. Abdou, Fabrication, structural elucidation, theoretical, TD-DFT, vibrational calculation and molecular docking studies of some novel adenine imine chelates for biomedical applications, *J. Mol. Liq.*, **2022**, 365, 119961.
2. H. K. Siuki, P. G. Kargar, G. Bagherzade, New Acetamidine Cu(II) Schiff base complex supported on magnetic nanoparticles pectin for the synthesis of triazoles using click chemistry, *Sci Rep.*, **2022**, 12, 3771.
3. A. A. Al-Shamry, M. M. Khalaf, H. M. A. El-Lateef, T. A. Yousef, G. G. Mohamed, K. M. Kamal El-Deen, M. Gouda, A. M. Abu-Dief, Development of New Azomethine Metal Chelates Derived from Isatin: DFT and Pharmaceutical Studies, *Materials*, **2023**, 16.
4. F. S. Aljohani, O. A. Omran, E. A. Ahmed, E. S. Al-Farraj, E. F. Elkady, A. Alharbi, N. M. El-Metwaly, I. O. Barnawi, A. M. Abu-Dief, Design, structural inspection of new bis(1H-benzo[d]imidazol-2-yl)methanone complexes: Biomedical applications and theoretical implementations via DFT and docking approaches, *Inorg. Chem. Commun.*, **2023**, 148, 110331.
5. A. M. Abu-Dief, Rafat M. El-Khatib, Faizah S. Aljohani, H. A. Al-Abdulkarim, S. Alzahrani, G. El-Sarrag, M. Ismael, Synthesis, structural elucidation, DFT calculation, biological studies and DNA interaction of some aryl hydrazone Cr<sup>3+</sup>, Fe<sup>3+</sup>, and Cu<sup>2+</sup> chelates, *Comp. Biol.Chem.*, **2022**, 97, 107643.
6. O. Bakhshi, G. Bagherzade, P. G. Kargar, Biosynthesis of Organic Nanocomposite Using Pistacia vera L. Hull: An Efficient Antimicrobial Agent, *Bioinorg. Chem. Appl.*, **2021**, 6, 1-18.
7. P. G. Kargar, G. Bagherzade, H. Beyzaei, S. Arghavani, BioMOF-Mn: An Antimicrobial Agent and an Efficient Nanocatalyst for Domino One-Pot Preparation of Xanthene Derivatives, *Inorg. Chem.*, **2022**, 61, 10678–10693.
8. A. Nameni, G. Bagherzade, M. Moudi, P. M. Kargar, Examination of the chemical profile of methanolic extract of Agaricus bisporus wild edible mushroom, Zarnagh region (East Azerbaijan province, Iran), *J. Hortic. Postharvest Res.*, **2022**, 5, 1-12.
9. E. Pormohammad, P. G. Kargar, G. Bagherzade, Loading of green-synthesized Cu nanoparticles on Ag complex containing 1,3,5-triazine Schiff base with enhanced antimicrobial activities, *Sci. Rep.*, **2023**, 13, 20421.
10. S. Azimi, M. S. Merza, F. Ghasemi, H. A. Dhahi, F. Baradarbarjastehbaf, M. Moosavi, P. M. Kargar, C. Len, Green and rapid and instrumental one-pot method for the synthesis of imidazolines having potential anti-SARS-CoV-2 main protease activity, *Sustain. Chem. Pharm.*, **2023**, 34, 101136.
11. M. Zubai, M. Sirajuddin, K. Ullah, A. Haider, F. Perveen, I. Hussain, S. Ali, M. N. Tahir, Synthesis, structural peculiarities, theoretical study and biological evaluation of newly designed O-Vanillin based azomethines, *J. Mol. Struct.*, **2020**, 1205, 127574.
12. H. Kargar, M. F. Mehrjardi, K. S. Munawar, Metal complexes incorporating tridentate ONO pyridyl hydrazone Schiff base ligands: Crystal structure, characterization, and applications, *Coord. Chem. Rev.*, **2024**, 501, 215587.
13. A. Varshney, D. Gupta, A. K. Choubey, S. Brahmchari, A. P. Mishra, Novel Schiff base ligand and its Co(II) & Cu(II) Metal complexes: Synthesis, Physicochemical Characterization, DNA Binding, and Antifungal Screening, *Mediterr. J. Chem.*, **2023**, 13(3), 219-227.
14. N. G. Yernale, M. B. H. Mathada, Preparation of octahedral Cu(II), Co(II), Ni(II) and Zn(II) complexes derived from 8-formyl-7-hydroxy-4-methylcoumarin: Synthesis, characterization and biological study, *J. Mol. Struct.*, **2020**, 1220, 128659.
15. P.G. kargar, G. Bagherzade, H. Beyzaei, A porous metal-organic framework (Ni-MOF): An efficient and recyclable catalyst for cascade oxidative amidation of alcohols by amines under ultrasound-irradiations, *Mol. Catal.*, **2022**, 526, 112372.
16. M. Amirasr, M. Rasouli, K. Mereiter, Copper(I) complexes of new N2S2 donor Schiff-base ligands derived from 1,2-bis-(2-amino-phenylsulfanyl)ethane, *Inorganica Chim. Acta*, **2013**, 404, 230-235.
17. R. Gup, B. Kirkan, Synthesis and spectroscopic studies of copper(II) and nickel(II) complexes containing hydrazonic ligands and heterocyclic coligand, *Spectrochim. Acta A Mol. Biomol.*, **2005**, 62, 1188-1195.

18. P. G. Kargar, S. Aryanejad, G. Bagherzade, Simple synthesis of the novel Cu-MOF catalysts for the selective alcohol oxidation and the oxidative cross-coupling of amines and alcohols, *Applied Organometallic Chemistry*, **2020**, 12, e5965.
19. A. U. Rani, N. Sundaraganesan, M. Kurt, M. Cinar, M. Karabacak, FT-IR, FT-Raman, NMR spectra and DFT calculations on 4-chloro-N-methylaniline, *Spectrochim. Acta A Mol. Biomol.*, **2010**, 75, 1523-1529.
20. H. Inac, M. Ashfaq, N. Dege, M. F. Dehneyebi, K. S. Munawar, N. K. Yağcı, E. P. Çınar, M. N. Tahir, Synthesis, Spectroscopic Characterizations, Single Crystal XRD, Supramolecular Assembly Inspection via Hirshfeld Surface Analysis, and DFT Study of a Hydroxy Functionalized Schiff base Cu(II) complex, *J. Mol. Struct.*, **2024**, 1295, 136751.
21. M. Dolaz, V. Mckee, S. Urus, N. Demir, A. E. Sabik, A. Gölcüd, M. Tümer, Synthesis, structural characterization, catalytic, thermal and electrochemical investigations of bidentate Schiff base ligand and its metal complexes, *Spectrochim. Acta A Mol. Biomol.*, **2010**, 76, 174-181.
22. A. Hosseinian, S. Jabbari, H. R. Rahimpour, A. R. Mahjoub, Synthesis and characterization of nano-scale of a new azido Co(II) complex as single and nano-scale crystals: Bithiazole precursor for the preparation of Co<sub>3</sub>O<sub>4</sub> nano-structures, *J. Mol. Struct.*, **2012**, 1028, 215-221.
23. H. Keypour, M. Shayesteh, R. Golbedaghi, A. Chehregani, A. G. Blackman, Synthesis, characterization, and X-ray crystal structures of metal complexes with new Schiff-base ligands and their antibacterial activities, *J. Coord. Chem.*, **2012**, 65, 1004-1016.
24. A. Kose, Synthesis, structural characterization and DNA binding properties of phthalazinylhydrazone-furan and triazolophthalazine-ferrocene compounds, *J. Mol. Struct.*, **2023**, 1274, 134471.
25. J. Saranya, S. J. Klubavathy, S. Chitra, A. Zarrouk, K. Kalpana, K. Lavanya, B. Ravikiran, Tetradentate Schiff Base Complexes of Transition Metals for Antimicrobial Activity, *Arab. J. Sci. Eng.*, **2020**, 6, 1-13.
26. M. Sirajuddin, S. Ali, M. N. Tahir, Organotin(IV) derivatives based on 2-((2-methoxyphenyl)carbamoyl)benzoic acid: Synthesis, spectroscopic characterization, assessment of antibacterial, DNA interaction, anticancer and antileishmanial potentials, *J. Mol. Struct.*, **2021**, 1299, 129600.
27. I. Ali, L.M.A. Mahmood, T. H. Mehdar, H. Y. Aboul-Enein, M. A. Said, Synthesis, characterization, simulation, DNA binding and anticancer activities of Co(II), Cu(II), Ni(II) and Zn(II) complexes of a Schiff base containing o-hydroxyl group nitrogen ligand, *Inorg. Chem. Commun.*, **2020**, 118, 108004.
28. H. A. Al-Abdulkarim, R. M. El-khatib, F. S. Aljohani, A. Mahran, A. Alharbi, G. A. M. Mersal, N. M. El-Metwaly, A. M. Abu-Dief, Optimization for synthesized quinoline-based Cr<sup>3+</sup>, VO<sup>2+</sup>, Zn<sup>2+</sup> and Pd<sup>2+</sup> complexes: DNA interaction, biological assay and in-silico treatments for verification, *J. Mol. Liq.*, **2021**, 339, 116797.
29. A. Varshney, A. P. Mishra, Synthesis, spectral characterization, computational studies, antifungal, DNA interaction, antioxidant and fluorescence property of novel Schiff base ligand and its metal chelates, *Spectrochim. Acta A Mol. Biomol.*, **2023**, 297, 122765.
30. P. G. Kargar, Z. Moodi, G. Bagherzade, F. Nikoomanesh: Synthesis, characterization, and antimicrobial activity of metal complexes derived from Schiff base of quercetin extracted from *Origanum vulgare* L., *Materials Chemistry and Physics*, **2024**, 317, 129207.
31. A. M. Abu-Dief, L. H. Abdel-Rahman, M. R. Shehata, A. A. Hassan Abdel-Mawgoud, Novel azomethine Pd (II)- and VO (II)-based metallo-pharmaceuticals as anticancer, antimicrobial, and antioxidant agents: Design, structural inspection, DFT investigation, and DNA interaction, *J Phys Org Chem.*, **2019**, 12, e4009.
32. S. A. Noghabi, P. G. Kargar, G. Bagherzade, H. Beyzaei, Comparative study of antioxidant and antimicrobial activity of berberine-derived Schiff bases, nitro-berberine and amino-berberine, *Heliyon*, **2023**, 9, e22783.